DC CONDUCTIVITY MEASUREMENTS IN SOLID STATE IONIC CONDUCTORS*

C.A.C. Sequeira
Laboratório de Electroquímica, Instituto Superior Técnico, Lisboa

ABSTRACT

There is currently a great deal of interest in solid electrolytes and mixed conductors due to their potential use in high performance battery or fuel cell systems and also because they can be employed in solid electrochemical transducers for a variety of scientific and technological purposes.
Due to the unusual range of behaviour of these materials and the special requirements related to their use, particular attention must be given to the problem of appropriate measurement and evaluation methods. One of the most useful characterization techniques for these "fast ionic conductors" is the dc measurement of their electrical conductivity. The concepts behind this approach and the dc measurement techniques of the total conductivity, the ionic conductivity and the electronic conductivity are given in this talk together with examples of its use employing solid electrolyte and mixed conductor samples which have a wider applicability in the area of materials research.

INTRODUCTION

Solid state ionic conductors are a relatively newly developed class of compounds which exhibit high ionic conductivities at fairly low temperatures below their melting points.
In the early stages of solid state ionics, high ionic conductivity was feasible only at high temperatures. This is the case of the stabilized zirconias, thorias and cerias which are well known as typical oxide ion conductors. Recently, however, the first outcome of development efforts was the discovery of Ag_3Si which has a high silver ionic conductivity at low temperature. Other solid electrolytes having high ionic conductivity at normal temperatures have been discovered, which include silver, copper, lithium, hydrogen, oxygen and sodium ionic conductors (1).
The main applications of these substances are in ion selective electrodes, chemical sensors, ion pumps, batteries and electrochemical

* Plenary lecture held at the 1st Meeting of the Portuguese Electrochemical Society, Coimbra, November 1984.

cells such as fuel cells, solid timers, potential memory cells, variable resistors and display devices. Table I shows some ionic & mixed conductors and their functional properties and uses. Consider for example the case of an oxygen ion conductor being used as an ion pump to separate oxygen from a mixture of oxygen and nitrogen:

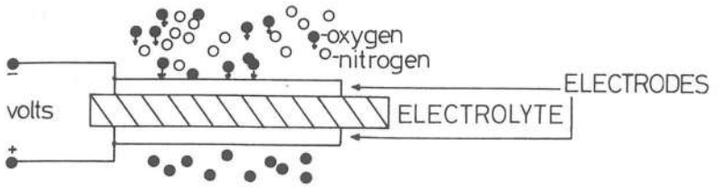

Fig. 1 Principle of a solid state ionic pump.

Due to the unusual range of behaviour of these materials and the special requirements related to their use, particular attention must be given to the problem of appropriate measurement and evaluation methods. It is unrealistic to expect that the approaches commonly used on more conventional materials can be casually employed on solid electrolytes and related materials with success.

One of the most useful characterization techniques for these "fast ionic conductors" is the direct measurement of their electrical conductivity. A particular problem arises with these materials in that on the application of a dc bias via two standard metal electrodes polarization occurs at the electrodes due to the inability of the mobile ions to cross the electrolyte/electrode interface and the ionic current falls to zero. In principle this problem may be solved in a variety of ways including the use of dc techniques with either a four electrode configuration or a cell configuration in which the sample is bounded by fully reversible/blocking interfaces which will allow ionic/electronic transport from electrolyte to electrode. However, in the two "reversible" electrode situation each type of electrode will only be applicable to one ionic species, may be difficult to identify and handle (e.g. molten alkali metals/salts for alkali ion battery electrolytes) and will probably not allow totally unhindered ionic motion across the interface. Four point methods are not always compatible with

TABLE I

IONIC AND MIXED CONDUCTORS

COMPOUND	MOBILE ION	SOME FUNCTIONAL PROPERTIES AND USES
$RbBiF_4$	F^-	Ion pumps for separation of fluorine. Fluoride ion selective electrodes
$LaCoO_3$, $PrCoO_3$, $NdCoO_3$	O^{2-}	Cathode materials in high temperature solid electrolyte fuel cells.
$La_4Co_3O_{10}$	O^{2-}	Oxygen electrochemical reduction catalyst.
$La_{0.5}Sr_{0.5}CoO_3$, $Nd_{0.8}Sr_{0.2}CoO_3$, $Nd_{0.5}Sr_{0.5}CoO_3$	O^{2-}	Oxygen electrode catalysts in aqueous alkaline solution batteries operating at ambient temperature. Cathode materials in high temperature solid electrolyte fuel cells. Oxygen sensor electrodes.
$(Bi_2O_3)_{0.83}(Y_2O_3)_{0.17}$	O^{2-}	Sensors under high oxygen partial pressures. Oxygen pumps.
$(ZrO_2)_{0.93}(Y_2O_3)_{0.07}$	O^{2-}	Electrolyte material in fuel cells, sensors and ion pumps.
$(ZrO_2)_{0.8}(Y_2O_3)_{0.2}(Yb_2O_3)_{0.04}$	O^{2-}	High temperature fuel and electrolysis cells.
$(CeO_2)_{0.93}(Gd_2O_3)_{0.07}$	O^{2-}	Sensors in atmospheres of intermediate oxygen partial pressure.
$SrYb_{0.5}Ce_{0.95}O_3$	H^+	High temperature fuel cell electrolyte material.
$HUO_2PO_4 \cdot 4H_2O$	H^+	Electrolyte for hydrogen fuel cells or water electrolyzers.
$RbAg_4I_5$	Ag^+	Electrolyte in long life secondary solid state batteries.
$AgI-Ag_4P_2O_7$	Ag^+	Electrochemical timing cells.
$Ag_6I_4WO_4$	Ag^+	Electrochemical potential memory cells. Solid state batteries for low rate discharge use.
$Rb_4Cu_{16}I_7Cl_{13}$	Cu^+	Solid state batteries.
$Na_2Sc_2P_3O_{12}$	Na	Solid state batteries. Ion selective electrodes.
$Na_3Zr_2Si_2PO_{12}$	Na^+	Advanced batteries
LiI.	Li^+	Cardiac pacemaker cells.
$LiI-Al_2O_3$ $LiCoO_2$	Li^+	Electrodes in lithium batteries.

specimen geometry and, unlike a.c. methods, only provide information about overall specimen properties. Although the dc methods present these difficulties, they are very successful under particular circumstances for a variety of purposes concerning bulk transport processes in both ionic and mixed conductors containing unusually mobile ionic species. The concepts behind this approach and the dc measurement techniques of the total conductivity, the ionic conductivity and the electronic conductivity are given in this talk together with examples of its use employing solid electrolyte and mixed conductor samples which have a wider applicability in the area of materials research.

DC MEASUREMENT OF THE TOTAL CONDUCTIVITY

When an electric field, $\dot{E}$, is applied across a crystal, a force is exerted on all the charged particles. If an ion or a defect has a charge q_i, the force F_i is given by

$$F_i = q_i \dot{E} \qquad /1/$$

This force causes a directional transport of the charged particles in addition to their random thermal motion. For long enough fields the resulting current density is given by

$$J_i = \sigma_i \dot{E} \qquad /2/$$

where σ_i is the conductivity of particles of type i. If a crystal contains different types of charged carriers, the total current density J is given by

$$J = \sigma \dot{E} \qquad /3/$$

where σ represents the total electrical conductivity, and is given by

$$\sigma = \sum_i \sigma_i \qquad /4/$$

Also σ_i is related to σ through

$$\sigma_i = t_i \sigma \qquad /5/$$

where t_i is called the transference or transport number of the species i. In a solid state ionic compound the total electrical conductivity is given by the sum of the electronic and ionic conductivities,

$$\sigma = \sigma_{ion} + \sigma_{el} = \sigma (t_{ion} + t_{el}) \qquad /6/$$

where t_{ion} and t_{el} represent the transference numbers of ions and electrons respectively.

Total conductivity values of an ionic solid MX can be obtained by a simple measurement of the relationship between the steady state charge flux and a steady applied electric potential difference between a pair of properly chosen electrodes in cell arrangements as follows:

M | MX | M (a)

M. M' | MX | M. M' (b)

M. MX | MX | M. MX (c)

M' | MX | M' (d)

X. M' | MX | M' X (e)

which can be represented by the simple equivalent circuit shown in Fig. 2.

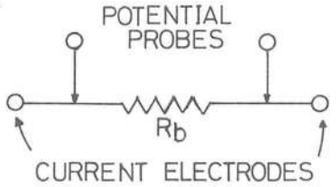

Fig. 2 Equivalent circuit representation of a two-point conductivity cell.

The electrodes in cell (b) and (c) are arranged to minimize the contact resistance between the electrode and the electrolyte (ionic solid) where M.M' means an alloy such as an amalgam. In order to minimize grain boundary effects of the electrolyte, the electrolyte must be pressure molded under several kbar. Cell (d) is used often when M is the alkali metal. In this case, Pt, Au or graphite is recommended as M'. Cell (e) is used when X^- is the mobile ion. In this case, X.M' (or M'.X) means a gas electrode made of porous metal inert to the ionic solid and gas.

Assuming that the electrodes maintain a constant composition across the sample and allow all common electrochemical species to cross the interface very rapidly, the total conductivity of the MX sample is

given by

$$\sigma = \frac{L}{A} \quad \frac{I}{V} \qquad /7/$$

where I and V are the current and voltage, and L and A are the length and constant cross sectional area. This two-point technique can be employed when one can neglect the sample-electrode interfacial impedance and the impedance of the electrode system itself relative to the impedance of the sample. The absence of concentration polarization and electrochemical effects at the sample-electrode interface must also be assumed. As a result, this method is only appropriate for interesting solid electrolytes when electrodes are used that are reversible both kinetically and thermodynamically for the mobile ionic species (2).

A variant on this technique, the four-point method, can sometimes be used when the sample-electrode interfacial impedance cannot be neglected. Steady state conditions are still assumed, so that the interfacial impedance must be time-independent. This technique is commonly used for measurements on solid conductors with predominant electronic conductivity (semiconductors), often employing a linear arrangement of four contacts. The outer two acting as current electrodes, and the inner pair for potential measurements.
A four-probe configuration is shown in Fig. 3a. The equivalent circuit representation is shown in Fig. 3b. Electrodes 1 and 4 are the active

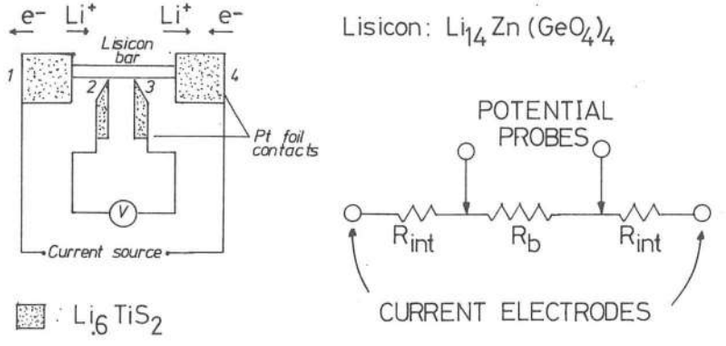

Fig. 3 Four-point conductivity cell and equivalent circuit representation(3).

(current carrying) electrodes at the ends of the sample. Electrodes 2 & 3 are equally spaced between the active electrodes and serve as potential electrodes. A small (~ 10 μ A) dc current is applied and maintained through the active electrodes and the potential difference V_{23} measured with a high impedance electrometer and recorded as a function of time. Under steady state conditions, the conductivity of a homogeneous sample with a flat surface is given by

$$\sigma = \frac{1}{2\pi d} \quad \frac{I}{V} \qquad /8/$$

where d is the distance between contacts. If the spacing between contacts is not uniform, σ becomes

$$\sigma = \frac{I}{2\pi V}\left[\frac{1}{d_1} + \frac{1}{d_3} - \frac{1}{d_1 + d_2} - \frac{1}{d_2 + d_3}\right] \qquad /9/$$

where d_1, d_2 and d_3 are the spacing values, d_2 being the distance between the two central potential probes.
Unless special attention is given to the establishment of proper conditions at the outer two contacts, this four-point dc method may not be useful for determining the total conductivity of materials in which ionic transport is appreciable. This is due to the requisite assumption that the sample-electrode impedance can be modeled as a simple time-independent and potential-independent resistance. In order for this to be true, the interfaces must act reversibly for both ionic and electronic species (3).
Two further statements should be made concerning the four-point technique. Potential measurements are made at points upon the surface, and may not be representative of the bulk if the sample is not homogeneous or if special phenomena occur at the surface that are not characteristic of the interior. Likewise, the method assumes that there is good communication between the surface and the inside. In materials with anisotropic crystal structures containing layers or tunnels, as is common among solid electrolytes, this assumption may not be obeyed, particularly in the case of single crystals.
In order to see how this is the case, consider a material with resistivities ρ_L and ρ_T parallel and perpendicular to the direction of current flow. By utilization of appropriate geometric factors, these values can be converted into longitudinal and transverse resistances R_L and R_T, and the measurement system represented by the equivalent circuit shown in Fig. 4. This figure neglects any

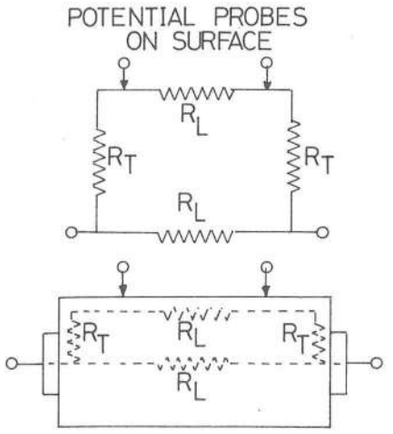

Fig. 4 Equivalent circuit of a measurement system containing an anisotropic sample.

interfacial impedances at the current electrodes.

This is a simple parallel circuit. For an applied voltage V, the current through the interior leg, I_{int}, is given by

$$I_{int} = \frac{V}{R_L} \qquad /10/$$

The current in the leg that includes communication between the interior and the surface through the transverse resistances, I_{ext}, is

$$I_{ext} = \frac{V}{R_L + 2R_T} \qquad /11/$$

The ratio of these currents I_{ext}/I_{int} is equal to the ratio of the potential difference measured between the potential probes on the surface and the actual potential difference across the interior portion of the sample:

$$\frac{I_{ext}}{I_{int}} = \frac{R_L}{R_L + 2R_T} \qquad /12/$$

If the sample is very anisotropic, so that $R_T \gg R_L$, this simplifies to

$$\frac{I_{ext}}{I_{int}} \simeq \frac{R_L}{2R_T} \qquad /13/$$

It is therefore quite evident that the actual longitudinal resistivity of a sample can be much greater than that inferred by the measurement of the potential difference between a pair of external probes in the four-point technique.

Similar difficulties may be encountered if the surface resistivity is a great deal lower than the bulk resistivity. This is an important consideration in the case of some semiconductors and dielectrics, but is often not important for solid electrolytes, due to their lower bulk resistivities (1-3).

In the investigation of the conductivity of new materials an important

parameter to be determined is the activation energy for conduction. Measurements of the sample conductivity at different temperatures are, therefore, necessary. The conductivity usually follows an Arrhenius equation and a plot of $\log \sigma T$ versus $1/T$ then leads to a straight line whose slope is simply related to the activation energy. The shape of the Arrhenius plot can also be used to determine phase transitions in ionic solids. This is a pertinent aspect, since a material is a solid electrolyte only when it is in a phase that possesses a structure conducive to ionic mobility.

The application of the above dc techniques is largely referred in the literature (4-12). Fig. 5 shows an apparatus used by Hooper (9) for dc conductivity measurements on high-density polycrystalline samples of Nazirpsio ceramic ($Na_3Zr_2PSi_2O_{12}$) in the range 120°-360 °C. The Nazirpsio pellet has a conductivity at 300 °C (Fig. 6) comparable to that of sodium β-alumina and is therefore a possible alternative electrolyte in Na/S cells, for example.

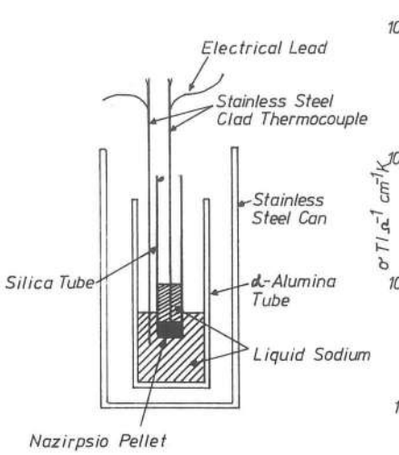

Fig. 5 Apparatus for dc conductivity measurements(9)

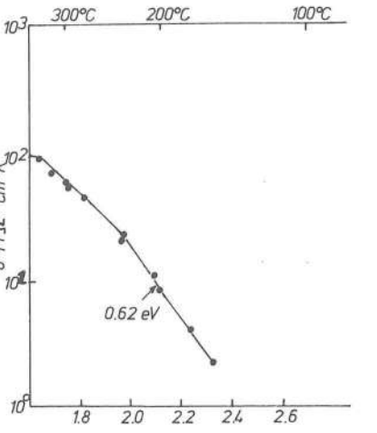

Fig. 6 Arrhenius plot for a Nazirpsio pellet(9)

Conduction characteristics of some LiI-Al_2O_3 solid materials are shown in Fig. 7. At an Al_2O_3 content ranging between 35 and 45 m/o,

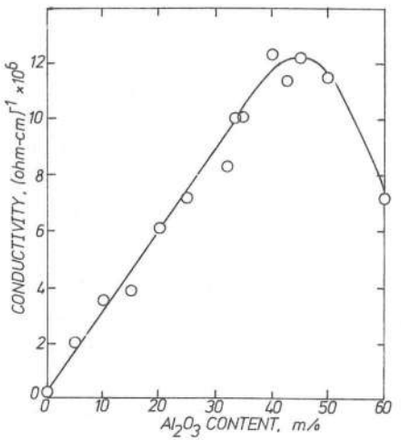

Fig. 7 Conductivity of the LiI(Al_2O_3) electrolyte vs. Al_2O_3 content(10)

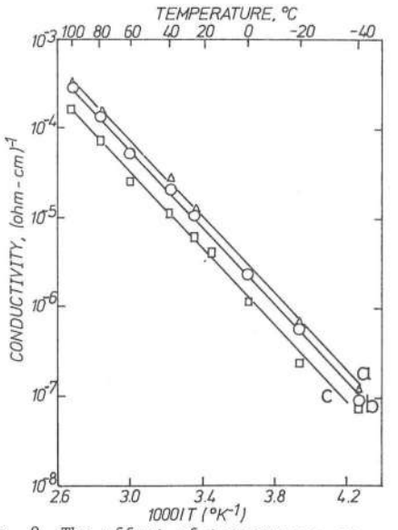

Fig. 8 The effect of temperature on the conductivity of the LiI (Al_2O_3) electrolyte. (a) 40m/o Al_2O_3; (b) 33m/o Al_2O_3; and 20m/o Al_2O_3(10)

the conductivity of this system can reach 10^{-5} ohm^{-1} cm^{-1} at room temperature (10). The apparent activation energy of the conduction process for the LiI--Al_2O_3 samples in the temperature range -40°-100°C was found to be 10kcal/mole (Fig. 8). Therefore, the LiI-40m/o Al_2O_3 electrolyte is suitable for high-energy solid-state battery systems using lithium anodes (10).

The temperature dependence of the electrical conductivities for samples in the $C_6H_{12}N_2$2RX--CuX system (R=H, CH_3, C_2H_5, X= Cl, Br, I) has been determined by Takahashi and Yamamoto (11). The results shown in Fig. 9 for 17CuCl.3$C_6H_{12}N_2$2HCl and 7CuBr.$C_6H_{12}N_2$2HBr exhibit an increasing activation energy at low temperature, which suggests that phase transitions occur near 65°C for 17CuCl.3$C_6H_{12}N_2$2HCl and 50°C for 7CuBr.$C_6H_{12}N_2$2HBr. However 7CuBr.$C_6H_{12}N_2$2HBr is conductive at room temperature and has a low activation energy of 3.3kcal/mole at 20°C. On the other hand, 17CuCl.3$C_6H_{12}N_2$2HCl has a high activation energy of 13.5 kcal/mole at 20°C, and it indicates that the conductive phase transfers to a nonconductive phase below 65°C

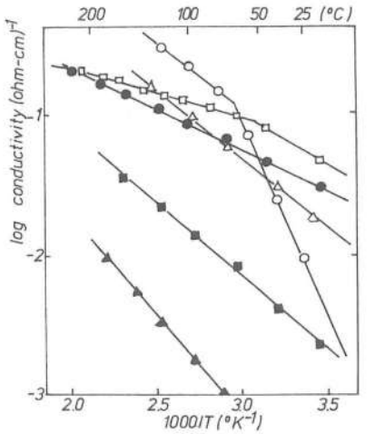

Fig. 9 Temperature dependence of the electrical conductivity of 17CuCl.3$C_6H_{12}N_2$2HCl (o), 4CuCl.$C_6H_{12}N_2$2CH_3Cl (Δ), 7CuBr.$C_6H_{12}N_2$2HBr (□), 47CuBr.3$C_6H_{12}N_2$2CH_3Br (●), 17CuBr.3$C_6H_{12}N_2$2C_2H_5Br (▲), and 17CuI.3$C_6H_{12}N_2$2CH_3I (■)(11)

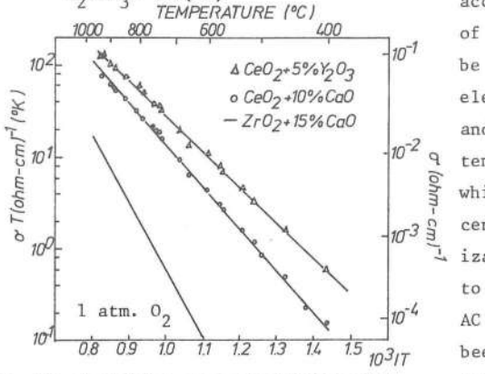

Fig. 10 Variation of conductivity with reciprocal absolute temperature for doped CeO_2 and comparison with data for CSZ.(12)

Data (12) for the variation of dc conductivity with temperature at $P(O_2)$=1 atm is shown in Fig. 10 for ceria doped with divalent and trivalent cations. Good straight lines are obtained in the log σT vs. 1/T plot for the range between 400°C and 1000°C. Also shown, for comparison, in Fig. 10 are data for calcia-stabilized zirconia (CSZ), the conductivity of which is at least a decade lower than for the two doped ceria samples in the range T < 900°C. For $(CeO_2)_{0.95}(Y_2O_3)_{0.05}$, because of its smaller activation energy, that factor increases to nearly 100 at 600°C and, accordingly, the question of whether doped CeO_2 can be useful as a solid oxide electrolyte for fuel cells and other applications at temperatures below those at which CSZ is useful then centers on whether polarization for CeO_2 is absent to lower temperatures. AC measurements have also been used to measure the conductivity of most of these systems and the results obtained by the ac/dc methods were nearly identical.

IONIC CONDUCTIVITY OF THE SOLID MATERIAL

The charge flux transported by ionic species across an ionic material can be measured by cell arrangements where a purely ionic conductor is introduced between the sample and electrodes. Examples are the cells (13, 14):

$$Ag \mid AgI \mid Ag_2S \mid AgI \mid Ag$$

$$O_2, Pt \mid ZrO_2(CaO) \mid \beta\text{-}Al_2O_3 \mid ZrO_2(CaO) \mid Pt, O_2$$

where the Ag | AgI and O_2, Pt | ZrO_2(CaO) systems act as electronically blocking electrodes, thus suppressing the electronic conductivity of the sample.

The ionic conductivity, σ_{ion}, is measured using a two-probe or four-probe dc method, as described for the total conductivity measurement. Special attention must be given to the establishment of proper conditions at the potential probes which, in the case of the four-probe technique, are located on the purely ionic conductor. Another dc method for the indirect measurement of the ionic conductivity utilizes the knowledge of the total conductivity of the sample and ionic transport number determinations, as discussed by the author in a recent publication (15). It is obvious from /5/ that

$$\sigma_{ion} = t_{ion}\,\sigma \qquad /14/$$

Fig. 11 shows the ionic conductivities of stabilized zirconias, thorias and cerias against the percentage of anionic vacancies at 1000°C (16). The thoria conductor shows p-type semiconduction at a high partial pressure of oxygen, and the ceria conductor exhibits n-type semiconduction at a low partial pressure of oxygen, suggesting that these conductors may be used as electrode materials for oxygen or hydrogen electrodes.

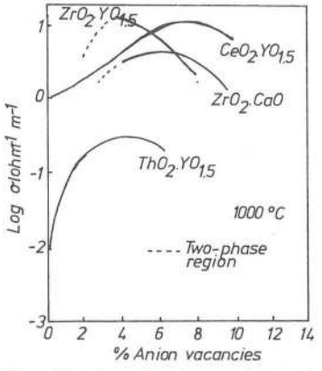

Fig. 11 Log (ionic conductivity) versus percentage anionic vacancies for selected fluorite solid solutions (16)

ELECTRONIC CONDUCTIVITY OF THE IONIC SOLID

The electronic conductivity of a solid material can be measured by a cell arrangement in which the sample itself is used as an electrolyte, bounded by two inert foreign metal electrodes acting as ionically blocking electrodes, e.g., Pt | Ag_2S | Pt (17), if the applied potential difference is less than the decomposition potential of the electrolyte. This arrangement, however, has the disadvantage that the chemical potentials of the components are not fixed.

A more satisfactory method that is particularly suitable for the determination of very low electronic conductivities is the Wagner asymmetric polarization cell method. Here the electrolyte sample MX (M^+ is a mobile ion) is contacted on one side by a parent metal electrode. This acts as a reversible electrode with known metal chemical potential. The second electrode consist of an inert metal like platinum which blocks the ionic flow. If an external dc potential E is applied in the direction indicated in Fig.12, the mobile ions in MX tend to move to the left, but since no metal can be replenished from the platinum electrode and X^- mobility is assumed negligible, this ionic current is soon blocked. In this stationary polarized state the ionic current is zero as long as the applied potential is lower than the decomposition potential of MX. The residual current indicated by the measuring instrument is then carried entirely by electrons and/or electron holes through the sample and is a measure of the electronic conductivity. According to Wagner (18), this current is given by

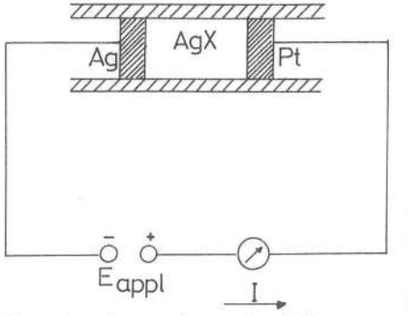

Fig. 12 Electronic conductivity measurement with a polarization cell.

$$I = I_e + I_h = \frac{RTA}{LF}\left\{\sigma_e^o\left[1 - \exp(-EF/RT)\right] + \sigma_h^o\left[\exp(EF/RT) - 1\right]\right\} \qquad /15/$$

where I_e and I_h represent the currents due to electrons and holes respectively; A and L are the cross-section area and the length of MX respectively; R is the gas constant; F, the Faraday constant; and T, the absolute temperature. The electronic conductivity due to electrons

and holes in MX in equilibrium with M are denoted by σ_e^o and σ_h^o respectively.

Under the conditions that the applied potential E is sufficiently high so that EF ≫RT and that one electronic carrier dominates, equation /15/ may be simplified to

$$I \simeq I_e \simeq \frac{RTA}{LF}\ \sigma_e^o \qquad \text{when } \sigma_e^o \gg \sigma_h^o \qquad /16/$$

$$I \simeq I_h \simeq \frac{RTA}{LF}\ \sigma_h^o\ \exp(FE/RT) \qquad \text{when } \sigma_e^o \ll \sigma_h^o \qquad /17/$$

According to equations /16/ and /17/ the polarization current, I, is independent of the applied potential in case of electron conduction while log I is a linear function of E in case of hole conduction. When the electrolytic species is an anion, a plot of lnI as a function of E should have a gradient of F/RT and an intercept of RTA σ_e^o/LF for electron conduction; for hole conduction, I should be independent of E. For many ionic solids, both electrons and holes act as carriers, in which case a plot of $(LFI/RTA)\left[\exp(FE/RT)-1\right]^{-1}$ against exp(-FE/RT) will have σ_e^o as the gradient and σ_h^o as the intercept for a mobile cation system and the reverse for a mobile anion system.

It should be noted that the value of σ_h^o obtained from the polarization experiment is that at zero applied potential. In other words, the leakage current calculated based on the σ_h^o value would be that of a cell whose open circuit voltage is zero such as M | MX | M. In actual electrochemical cells, the open circuit voltage is not zero. Therefore, the actual leakage current is higher than that calculated from σ_h^o (19, 20) inasmuch as the concentration of hole carriers increases exponentially with the electrode potential.

In view of the cell voltage effect on the electronic conductivity due to electron holes, the electronic conductivity must be considered in relation to the cell voltage in the selection of ionic solids. For example, PbF_2 is a hole conductor and its σ_h^o value is extremely low ($< 10^{-20}$ ohm^{-1} cm^{-1}) in comparison with the ionic conductivity (10^{-6} - 10^{-8} ohm^{-1} cm^{-1}); so, one would expect PbF_2 to be a suitable solid electrolyte material. However, Kennedy (20) has concluded that PbF_2 is suitable as a solid electrolyte only if the cell voltage is less than 1.5V. The same author (20) has also pointed out that the transport number of electrons, t_{el}, is lower in a battery than in the

Wagner cell, whereas the reverse applies to t_h.

Liang, Joshi and Hamilton (19) have proposed, based on their investigation of the solid state storage battery systems, that the leakage current should be measured directly at the voltage of the electrochemical cell under investigation. It was found that σ_{ion} of LiI dispersed in Al_2O_3 was 10^{-4} ohm^{-1} cm^{-1} at room temperature and 10^{-1}ohm^{-1} cm^{-1} at 300°C (Fig. 13). The electronic conductivity of the $LiI(Al_2O_3)$ electrolyte was found to be due to hole carriers & the σ_h^o values were less than 10^{-40} ohm^{-1} cm^{-1} and 5×10^{-27} ohm^{-1} cm^{-1} at room temperature and 300°C respectively. However, at the voltage of the solid state storage cells such as Li-Si/$LiI(Al_2O_3)$/TiS_2, Li/$LiI(Al_2O_3)$/TaS_2 and Li-Si/$LiI(Al_2O_3)$/TiS_2, Sb_2S_3, Bi which is about 2.5V, the leakage current (Fig. 14) due to the electron holes was found to be

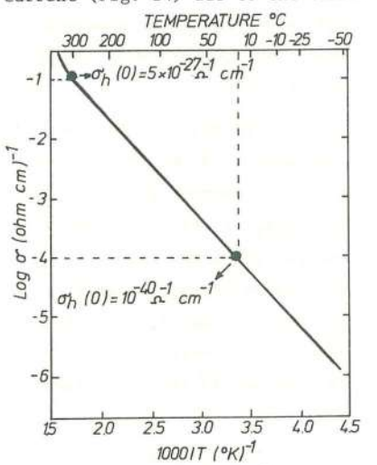

Fig. 13 Ionic conductivity of $LiI(Al_2O_3)$ as a function of temperature.(19)

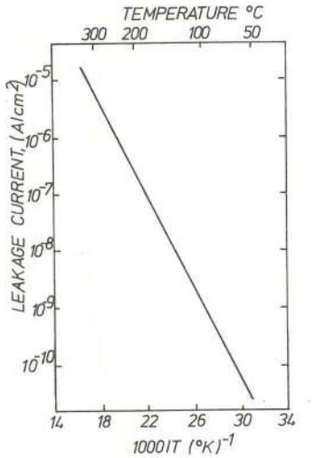

Fig. 14 Electronic leakage current of a 0.05 cm thick $LiI(Al_2O_3)$ solid electrolyte layer at 2.5V.(19)

significantly higher than that calculated from the σ_h^o values. Nonetheless, the leakage current was still low enough to be considered negligible in comparison with the current capability of the solid state storage cells. Accordingly, it was concluded that $LiI(Al_2O_3)$ is a practical solid electrolyte material.

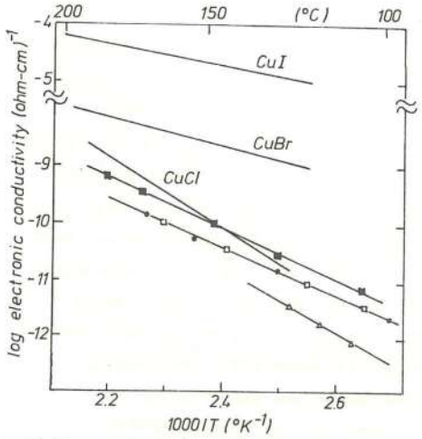

Fig. 15 Temperature dependence of the electronic conductivity of copper (I) halides, $4CuCl.C_6H_{12}N_2 2CH_3Cl$ (Δ), $7CuBr.C_6H_{12}N_2 2HBr$ (□), $47CuBr.3C_6H_{12}N_2 2CH_3Br$ (•), and $17CuI.3C_6H_{12}N_2 2CH_3I$ (■).(11)

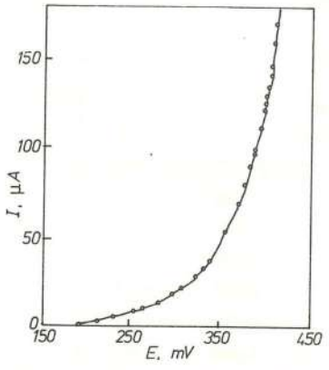

Fig. 16 I vs. E for a KCu_4I_5 pellet (L/A = 0.184 cm^{-1}) at 281.5 °C.(8)

The electronic conductivity of the $C_6H_{12}N_2 2RX$-CuX system was measured by Wagner's polarization method (Fig. 15). The current vs. cell voltage curves for the cell, Cu/sample/graphite, showed a quasi-exponential increase of current in the temperature range of 100°C-200°C for all samples investigated. Therefore, according to Wagner's theory, the hole conduction may be assumed to be dominant under this experimental condition (11).

The results obtained by Bonino and Lazzari (8) at 281.5°C by forcing a current I through a $Cu/KCu_4I_5/Pt$ cell (Pt being the positive) and measuring the steady state voltage E are reported in Fig. 16. The experimental points follow satisfactorily (Fig. 17) the equation:

$$\log I = \log \sigma_h^o \, (ART/LF) + \log \left[\exp (EF/RT) - 1\right] \quad /19/$$

from where a value of 2×10^{-7} $ohm^{-1}cm^{-1}$ for σ_h^o is calculated at 281.5 °C.

Measurements of the partial conductivities of electronic carriers in $Cu_{16}Rb_4Cl_{13}I_7$ and $Cu_{16}Rb_4Cl_{12}I_8$ carried out with the aid of asymmetric dc polarization

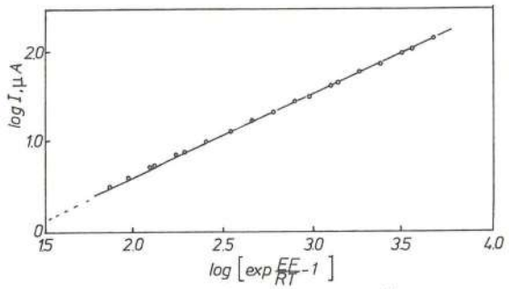

Fig. 17 Log I vs. log $\left[\exp (EF/RT) - 1\right]$ for a KCu_4I_5 pellet (L/A = 0.184 cm^{-1}) at 281.5 °C.(8)

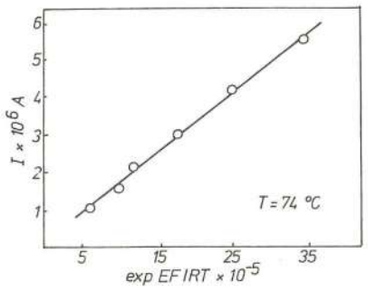

Fig. 18 Current vs. exp EF/RT for $Cu_{16}Rb_4Cl_{12}I_8$ with Pt ion blocking electrode at 74°C

cells of the type: Cu, CuCl, CuI $|Cu_{16}Rb_4I_{7+x}Cl_{20-(7+x)}|$ Pt or graphite, were dealt with by Chaney et al. (21). Values of the hole conductivity were determined from the slope of exp(EF/RT)-1 vs. I plots, in preference to determining values from the intercepts, because greater accuracy could be achieved (see Fig. 18).

Wagner's method has been much used to study σ_{el}, but pulse techniques are now coming onto prominence. A technique based on the fact that electronic carriers can respond more rapidly than ionic carriers to fluctuations in the applied potential has been suggested by Yakoto (22) in which a dc voltage is applied across an electrolytic cell incorporating two similar working electrodes, e.g., M | MX | M. The current-time characteristics are monitored as a rapid voltage pulse is superimposed. If electronic conductivity is insignificant, then the slow response time of the ions will cause a smooth rise to the new current plateau corresponding to the higher voltage level and a similar smooth decline when the voltage pulse is removed. If on the other hand there is an electronic contribution, the smooth rises and falls will be preceded by abrupt jumps. This method has been recently developed (23), and transient currents arising from the redistribution of electronic carriers and the motion of ions in CuI have been studied.

Lack of space does not allow a further analysis of this subject. Never-

theless, most of the concepts and problems associated with the dc conductivity measurements in solid state ionic conductors have been discussed, as was our purpose, and their importance in the area of materials research has been highlighted.

ACKNOWLEDGMENT

I wish to thank my wife, Maria Elisa, for her drawing of the figures and table.

REFERENCES

1. P. Hagenmuller and W. Van Gool (Eds.), "Solid Electrolytes", Academic Press, Inc., New York (1978).
2. G.D. Mahan and W.L. Roth (Eds.), "Super Ionic Conductors", Plenum Press, New York (1976).
3. R.D. Armstrong (Ed.), "Solid Ionic and Ionic-Electronic Conductors", Pergamon Press Ltd., Oxford (1977).
4. J. Singer, W.L. Fielder, H.E. Kautz, and J.S. Fordyce, J. Electrochem. Soc. 123, 614 (1976).
5. S. Geller, P.M. Skarstad, and S.A. Wilber, J. Electrochem. Soc., 122, 332 (1975).
6. T. Kudo and H. Obayashi, J. Electrochem. Soc. 122, 142 (1975).
7. P.V. Wright, Br. Polym. J. 7, 319 (1975).
8. F. Bonino and M. Lazzari, J. Power Sources 1, 103 (1976/77).
9. A. Hooper, J. Electroanal. Chem. 109, 161 (1980).
10. C.C. Liang, J. Electrochem. Soc. 120, 1289 (1973).
11. T. Takahashi and O. Yamamoto, J. Electrochem. Soc. 122, 83 (1975).
12. H.L. Tuller and A.S. Nowick, J. Electrochem. Soc. 122, 255 (1975).
13. M. Hebb, J. Chem. Phys. 20, 185 (1952).
14. M.S. Whittingham and R.A. Huggins, J. Chem. Phys. 54, 414 (1971).
15. C.A.C. Sequeira and A. Hooper (Eds.), "Solid State Batteries", Martinus Nijhoff Publishers, The Hague, to be published.
16. T.H. Etsell and S.N. Flengas, Chem. Rev. 70, 339 (1970).
17. N.F. Mott and R.W. Gurney (Eds), "Electronic Processes in Ionic Crystals" Oxford University Press, London (1950).

18. C. Wagner, International Committee of Electrochemical Thermodynamics and Kinetics. Proc. 7th Meeting (1955), Butterworths, London (1956).
19. C.C. Liang, A.V. Joshi and N.E. Hamilton, J. Appl. Electrochem. 8, 445 (1978).
20. J.H. Kennedy, J. Electrochem. Soc. 124, 865 (1977).
21. C. Chaney, D.F. Shriver and D.H. Whitmore, Solid State Ionics 5, 505 (1981).
22. I. Yakoto, J. Phys. Soc. Jpn 8, 595 (1953).
23. P. Vashishta, J.N. Mundy and G.K. Shenoy (Eds), "Fast Ion Transport in Solids", page 581, North-Holland, New York (1979).